First European Conference on Earthquake Engineering and Seismology
(a joint event of the 13th ECEE & 30th General Assembly of the ESC)
Geneva, Switzerland, 3-8 September 2006
Paper Number: 1245

NUMERICAL ANALYSIS OF GEO-STRUCTURES IN A LIQUEFACTION REGIME

Konstantinos ANDRIANOPOULOS[1], Achilleas PAPADIMITRIOU[2] and George BOUCKOVALAS[3]

SUMMARY

A new numerical methodology is presented for the simulation of the non cohesive soil response under small, medium and large cyclic strains, with special interest given to liquefaction phenomena. The new methodology is based on a recently proposed elastoplastic Bounding Surface model, which has been implemented to the finite difference code *FLAC*, via its User-Defined-Model capability. The new methodology is calibrated against element tests on Nevada sand, while the simulation of centrifuge model tests from the VELACS project validates its applicability to boundary value problems. Using this well established methodology, numerical analyses are performed, for the common case of a thin clay cap overlying a liquefiable sand layer, in order to provide insight to the mode of failure due to earthquake-induced liquefaction of the subsoil.

1. INTRODUCTION

The simulation of soil response during a strong earthquake is still a subject of significant research in the field of Geotechnical Earthquake Engineering. The bulk of this research is performed via numerical analysis, which can deal with complicated situations where simple analytical solutions are too crude. The very large majority of currently available constitutive models implemented in commercial codes oriented towards Geotechnical Engineering are not able to quantitatively capture this response. This is mainly due to the complicated nature of this response. In particular, features of this response like the accumulation of permanent deformations, the degradation of soil moduli, the increase of hysteretic damping and the evolution of soil fabric as a function of imposed cyclic shear strains require advanced constitutive modeling, which may prove difficult if not impossible to implement in commercial codes. Most often the solution to this problem is given via in-house codes, which are developed in various research institutes and universities and are not readily available to the technical community and have sometimes a narrow range of applicability.

This paper presents the implementation and validation of a new user defined model for cyclic loading in *FLAC* [Itasca, 1998]. This model takes advantage of the UDM (User-Defined Model) capability and has been developed with the aim to overcome the above shortcomings. It is based on incremental elasto-plasticity and aims at performing realistic fully coupled dynamic analyses for practical problems of Geotechnical Earthquake Engineering.

2. SAND PLASTICITY MODEL

The new UDM [Andrianopoulos, 2006] is a bounding surface model with a vanished elastic region that incorporates the framework of Critical State Theory. It is based on a recently proposed model [Papadimitriou et

[1] Ph.D. Candidate, Geotechnical Dept., School of Civil Engineering, National Technical University of Athens, 15780, Zografou, Greece
Email : kandrian@central.ntua.gr
[2] Research Fellow, Geotechnical Dept., School of Civil Engineering, National Technical University of Athens, 15780, Zografou, Greece
Email : loupapas@alum.mit.edu
[3] Professor, Geotechnical Dept., School of Civil Engineering, National Technical University of Athens, 15780, Zografou, Greece
Email: gbouck@central.ntua.gr

al., 2001; Papadimitriou & Bouckovalas, 2002], which has been developed with the ambition to simulate the cyclic behavior of non-cohesive soils (sands and silts), under various (small-medium-large) cyclic strain amplitudes and various initial stress and density conditions, using a single, sand-specific set of parameters. Extensive comparison with laboratory test results has shown that this goal has been achieved to a good extent, since many basic aspects of cyclic soil behavior, such as the generation of excess pore water pressures towards liquefaction, permanent deformations, shear-induced dilation, softening and the effects of evolving fabric anisotropy are well simulated.

In its current form, the model incorporates three open cone-type surfaces with apex at the origin of stress space: (i) the critical state surface at which deformation develops for fixed stresses and zero volumetric strain, (ii) the bounding surface which locates the peak stress ratio states and (iii) the dilatancy surface which dictates the sign of volumetric strain increment during loading. The shape of these surfaces is firstly presented in the triaxial [q-p] space with the aid of Figure 1, while the shape of the model surfaces in the π-plane of the deviatoric stress space is presented in Figure 2.

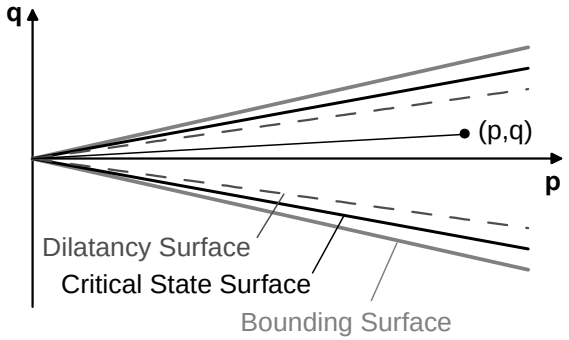

Figure 1 Model surfaces in the triaxial (q-p) space

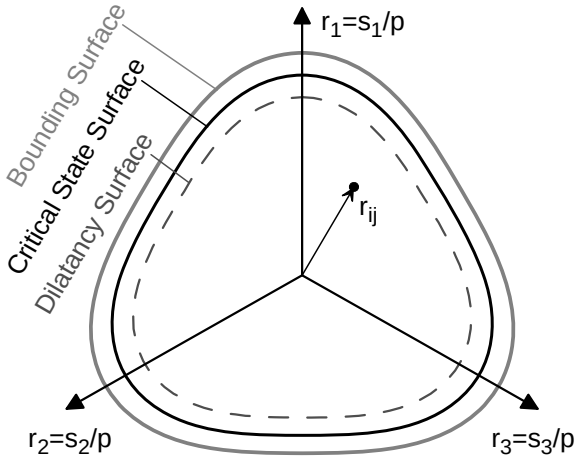

Figure 2 Model surfaces in the π-plane of the deviatoric stress space

Its basic feature is the direct association of shear behavior to the state parameter ψ [Been and Jefferies, 1985], which is defined with respect to a unique critical state line (CSL) or steady state line (Fig. 3). This is accomplished by introducing ψ explicitly in constitutive equations, i.e. by correlating the position of model surfaces at every step with the constantly changing value of the state parameter.

The non-linear soil response under small to medium cyclic strain amplitudes is simulated mainly by introducing a Ramberg-Osgood-type hysteretic formulation in a manner similar to the paraelastic theory of Hueckel & Nova (1979). At larger cyclic strain amplitudes elastoplasticity governs the behavior and a properly defined scalar-valued variable is introduced, which reflects macroscopically the effect of fabric evolution during shearing on the plastic modulus.

Note that there is no purely elastic region and thus the response of soil during loading is continuously elastoplastic, i.e. irrecoverable deformations occur at every incremental step. The choice of a vanished elastic region provides a smoother transition from smaller to larger strains, from para-elastic to fully elastoplastic behavior, and hence improves the numerical robustness and efficiency of the code (Naylor 1985, Andrianopoulos 2006). In this way, it was possible to satisfactorily resolve a number of issues that significantly increase the required computational effort, i.e. the stress point crossing of the yield surface, the drift correction resulting from the weak enforcement of the consistency condition, and the subsequent sub-stepping in the integration scheme. The adoption of a vanished yield surface differentiates the proposed model from the original of Papadimitriou & Bouckovalas (2002), as it lead to a number of other modifications as well, namely: (i) introduction of a new mapping rule [Andrianopoulos et al., 2005], and (ii) modification of the existing interpolation rule. However, the basic equations were preserved, so that the reader can readily refer to the original publication for more details.

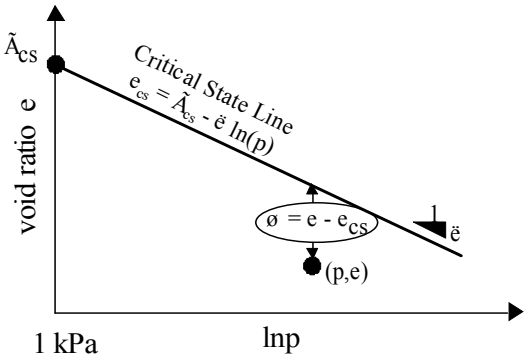

Figure 3 Critical State Line and state parameter ψ in e-lnp space

3. IMPLEMENTATION IN FLAC

The way in which constitutive equations are integrated at each calculation step dictates the accuracy of the computations, especially when complex constitutive models are involved such as the one presented in this paper. For this purpose, various numerical techniques - implicit, explicit and semi-explicit - which satisfy the aforementioned accuracy criterion have already been proposed in the literature. Naturally, the choice for the most efficient algorithm depends on the constitutive law and the numerical code where it has been implemented.

The aforementioned constitutive model was incorporated in the code *FLAC*, using the UDM capability. In the current work, the sub-stepping technique with automatic error control originally proposed by Sloan et al. (2001) was adopted, which belongs to the family of effective explicit algorithms. In brief, this algorithm divides automatically the applied strain increment into sub-increments, using an estimate of the local error, and attempts to control the global integration error in the computed stresses. It uses a modified Euler scheme and consists of two basic steps:

In the first step, a first approximation to the stress increment $\Delta\sigma_1$ is calculated by using the initial matrix of elastoplastic moduli:

$$\Delta\sigma_1 = D_{ep}(\sigma_{n-1,} H_{n-1}) \, \Delta\varepsilon_n \tag{1}$$

$$\Delta H_1 = \Delta\lambda(\sigma_{n-1,} H_{n-1}, \Delta\boldsymbol{\varepsilon}_n) \, B(\sigma_{n-1}) \tag{2}$$

where D_{ep} is the matrix of elastoplastic moduli, σ_{n-1} & H_{n-1} are the stress tensor and hardening parameters respectively at end of the previous increment, $\Delta\varepsilon_n$ is the given strain increment at current step and $\Delta\lambda$ is a scaling loading index. In the second step, the matrix of elastoplastic moduli D_{ep} is temporarily updated and a new approximation of the stress increments is calculated, as:

$$\Delta\sigma_2 = D_{ep}(\sigma_{n-1} + \Delta\sigma_{1,} H_{n-1} + \Delta H_1) \, \Delta\varepsilon_n \tag{3}$$

$$\Delta H_2 = \Delta\lambda(\sigma_{n-1}+\Delta\sigma_1, H_{n-1}+\Delta H_1, \Delta\boldsymbol{\varepsilon}_n) \, B(\sigma_{n-1}+\Delta\sigma_1) \tag{4}$$

Consequently, the relative error between these two approximations is estimated and, if required, sub-stepping is activated. The size of each sub-step is continuously updated so that the relative error is less than a specified tolerance level. At the end of each successful sub-step, the stress increment is computed according to:

$$\Delta\sigma_n = ½ (\Delta\sigma_1 + \Delta\sigma_2) \quad (5)$$

$$\Delta H_n = ½ (\Delta H_1 + \Delta H_2) \quad (6)$$

It is noted that, due to the solution scheme used in *FLAC* (explicit time marching scheme), the use of small increments are a prerequisite for the stability of computations. Thus, the majority of solution steps (e.g. for $\Delta\varepsilon < 10^{-4}$) lead to relative errors that are below the usually adopted tolerance levels and hence no sub-stepping is needed. However, given that explicit integration schemes are only conditionally stable and that the proposed model is highly non-linear and strongly path-dependent, a more elaborate technique is needed, which will ensure the stability of the computations. This is especially true when dynamic coupled analysis is performed as well as at instances where soil behavior turns from contractive to dilative or unloading follows dilation. The integration procedure is greatly enhanced when a sub-stepping technique is adopted and this is especially with (a) the modified Euler two-step approach and (b) a vanished yield surface region where no enforcement of consistency condition is needed that would leads to round-off errors.

4. SAND MODEL CALIBRATION

In the present study, the parameters of the model are calibrated on the basis of data from element laboratory tests performed on fine Nevada sand at relative densities of D_r = 40 & 60% and initial effective stresses between 40 and 160 kPa [Arulmoli et al., 1992]. In particular, the data originate from resonant column tests as well as direct simple shear and triaxial tests. Thus, they offer a quantitative description of various aspects of non-cohesive soil response under cyclic loading, such as shear-modulus degradation and damping increase with cyclic shear strain, liquefaction resistance and cyclic mobility. Results from this calibration are presented in Figures 4 through 8.

Namely, Figure 4 presents an one-to-one comparison of the model predictions with the respective data for a typical undrained simple shear test at D_r = 40% and initial effective stress $\sigma'_{v,o}$ = 80 kPa. Similarly, Figure 5 presents a one-to-one comparison for a typical cyclic undrained simple shear test at D_r = 40% and initial effective stress $\sigma'_{v,o}$ = 80 kPa, where significant excess pore pressures develop leading to liquefaction. In addition, Figure 6 presents the overall comparison for cyclic shearing under small and medium strain amplitudes, in terms of maximum shear modulus G_{max} and its subsequent degradation with cyclic shear strain amplitude γ_{cyc}(%) as well as the increase of hysteretic damping ξ(%). Finally, Figures 7 & 8 present the overall comparison of model predictions to test data for large strain amplitudes, where the subsequent buildup of excess pore pressures dictates the response. The relevant comparisons are made in terms of the excess pore pressure during the first cycle Δu_1 and the number of cycles required to reach complete liquefaction N_L for a given cyclic stress ratio CSR.

5. VERIFICATION OF METHODOLOGY IN BOUNDARY VALUE PROBLEMS

The proposed numerical methodology has been validated against results from the well-known VELACS experimental project [Arulmoli et al., 1992]. In particular, results from Model tests No. 1 and No. 2 were used that simulate the one-dimensional (1D) response of a liquefiable soil under level and mildly sloping sites respectively. Furthermore, model test No. 12 was used, which simulates the response of shallow foundations on liquefiable soils. Due to length limitations, this paper presents the results from the last validation run.

The test arrangement and the instrumentation for Model test No. 12 are shown in Figure 9. In prototype scale, the experiment refers to a 6 m deep Nevada Sand layer with 60% relative density, overlaid by a 1 m deep Bonnie Silt layer, with the ground water surface at 1 m above the silt surface. A 4 m tall and 3 m wide rigid square structure is seated at the center of the sample, 0.5 m below the surface of the sand layer, inducing an average bearing pressure of 150 kPa.

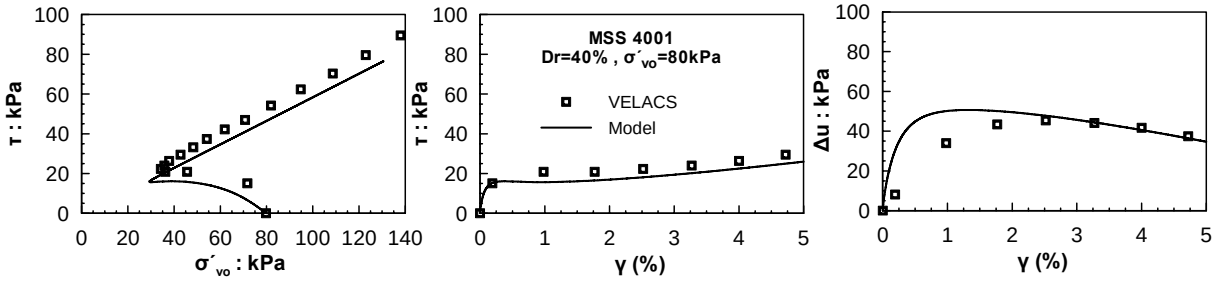

Figure 4 Exemplary comparison of simulation to data for a monotonic undrained simple shear test

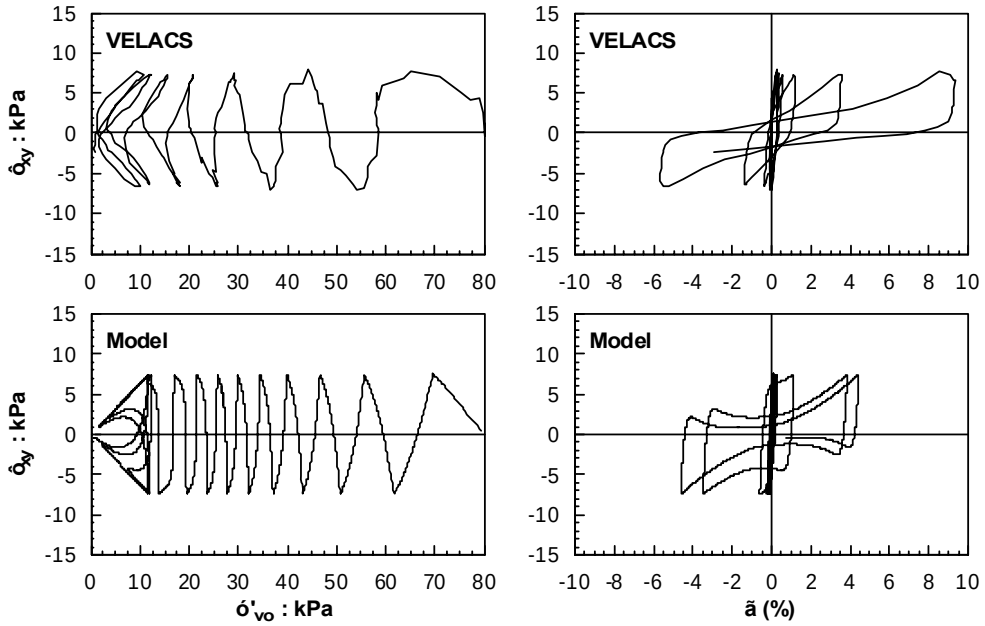

Figure 5 Exemplary comparison of simulation to data for a cyclic undrained simple shear test

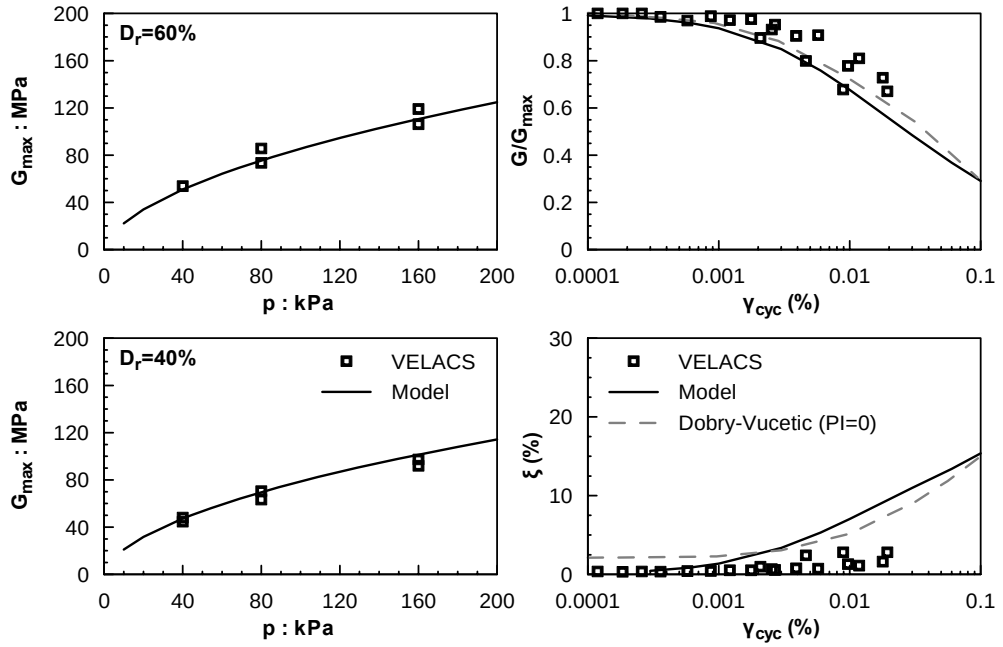

Figure 6 Summary comparisons of simulations versus data for cyclic shearing in terms of the maximum shear modulus G_{max} values and the G/G_{max}-γ_{cyc} degradation and the ξ-γ_{cyc} increase curves

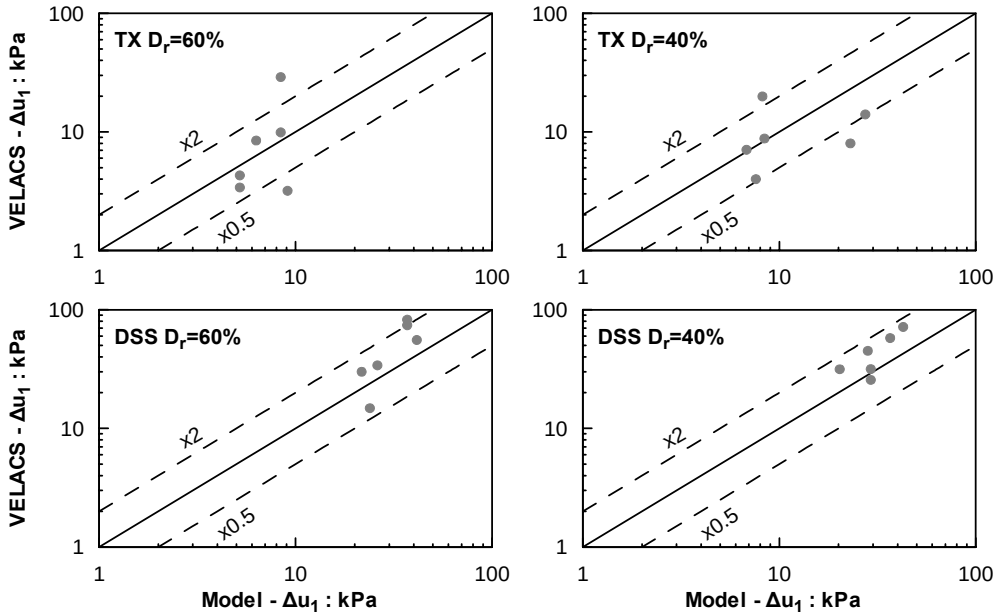

Figure 7 Summary comparisons of data versus simulations for cyclic shearing in terms of Δu_1.

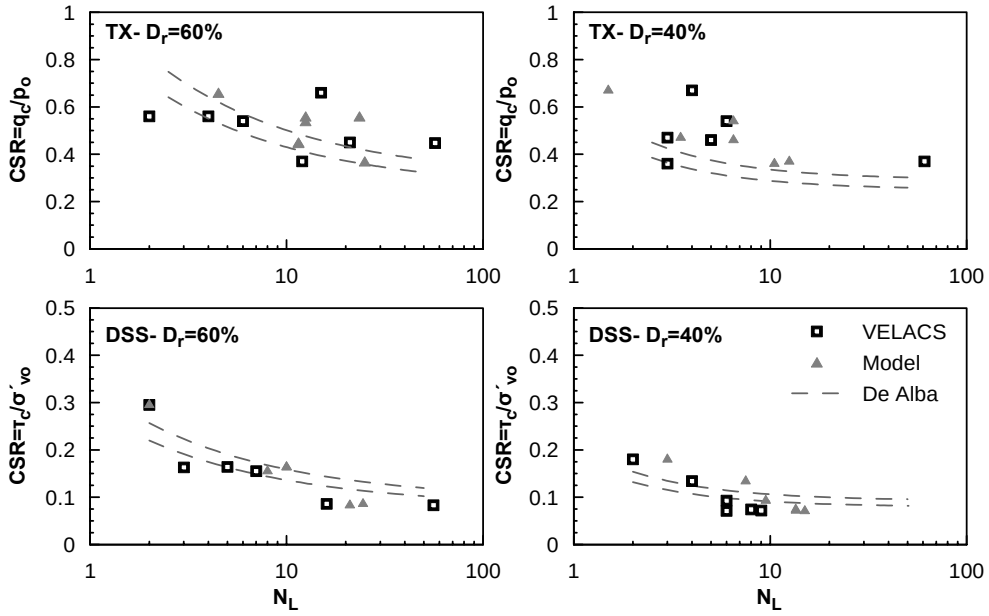

Figure 8 Summary comparisons of data versus simulations for undrained cyclic shearing in terms of the number of cycles N_L for initial liquefaction.

The centrifuge model was built inside a rigid box with an inside plan area of 282 mm × 128 mm and tested at 100 g centrifugal acceleration. The input motion consisted of ten (10) more or less uniform cycles of horizontal acceleration with 0.25 g amplitude and 2 Hz frequency (Fig. 10). The vertical acceleration during the experiments was minimal and was not taken into account during the numerical simulation. The response of the ground and the structure was monitored with three (3) accelerometers (AccB, AccC and AccD), located at different depths under the foundation, three (3) pore pressure transducers (PPT1, PPT2 and PPT3) also located under the foundation, one (1) pore pressure transducer (PPT4) placed in the free field. Furthermore, one (1) LVDT monitored the settlement of the structure. The grid used for the numerical analysis is shown in Figure 9. The element size varied from 0.75 m × 0.5 m at the vicinity of structure to 1.5 m × 1.0 m far from it. Acceleration was applied both at the bottom and the lateral boundaries in order to simulate the rigid box device. No interface elements were used between the structure and the rest of the grid. The Bonnie silt layer was simulated by using a simplified version of the proposed model, which includes only the Ramberg-Osgood

hysteretic type stress-strain relation appropriately calibrated to simulate the cyclic response of a fine soil with plasticity index PI = 15%.

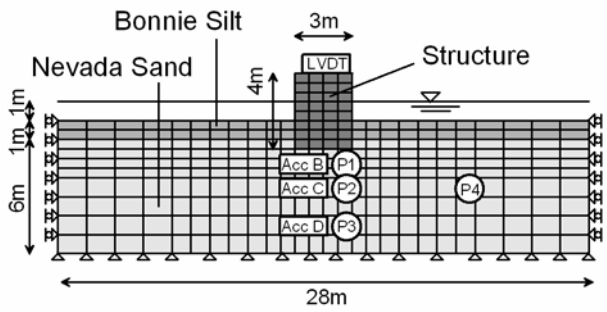

Figure 9 VELACS Model 12 configuration - Mesh and boundary conditions.

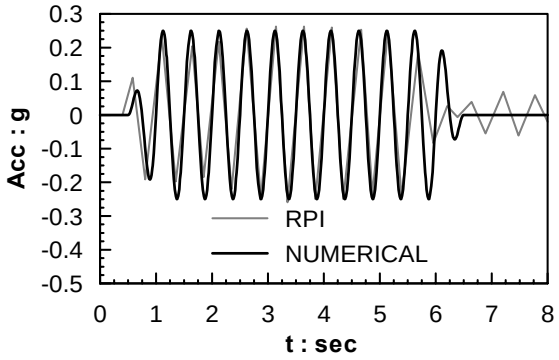

Figure 10 Specified and actual input motion.

Figure 11 presents the excess pore pressure ratio $r_u = \Delta_u/\sigma'_{vo}$ contours and flow vectors derived from the analysis during dynamic loading, whereas Figure 12 compares the relevant numerical predictions and centrifuge test recordings. Pore pressure transducer PP4 is representative of the conditions away from structure, i.e. the free-field conditions, where liquefaction is observed after approximately 4 seconds of shaking. Transducers PP1, PP2 and PP3, at the vicinity of the structure show that its presence prevents soil from liquefying.

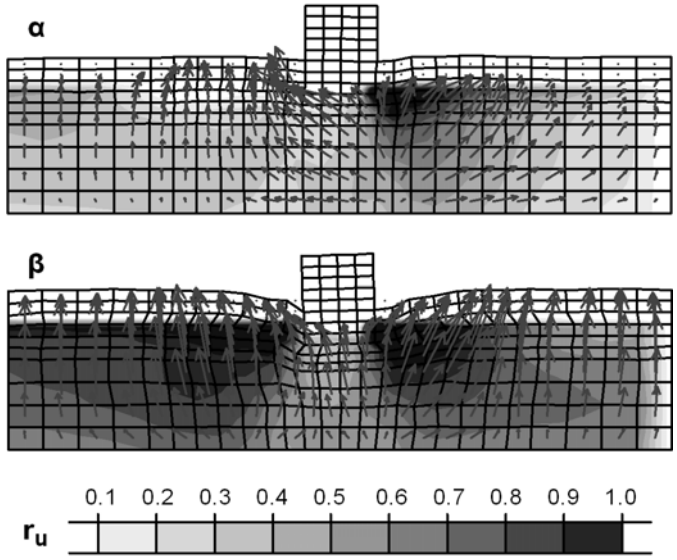

Figure 11 Excess pore pressure ratio contours and flow vectors from analyses for (a) t=2sec & (b) t=5sec

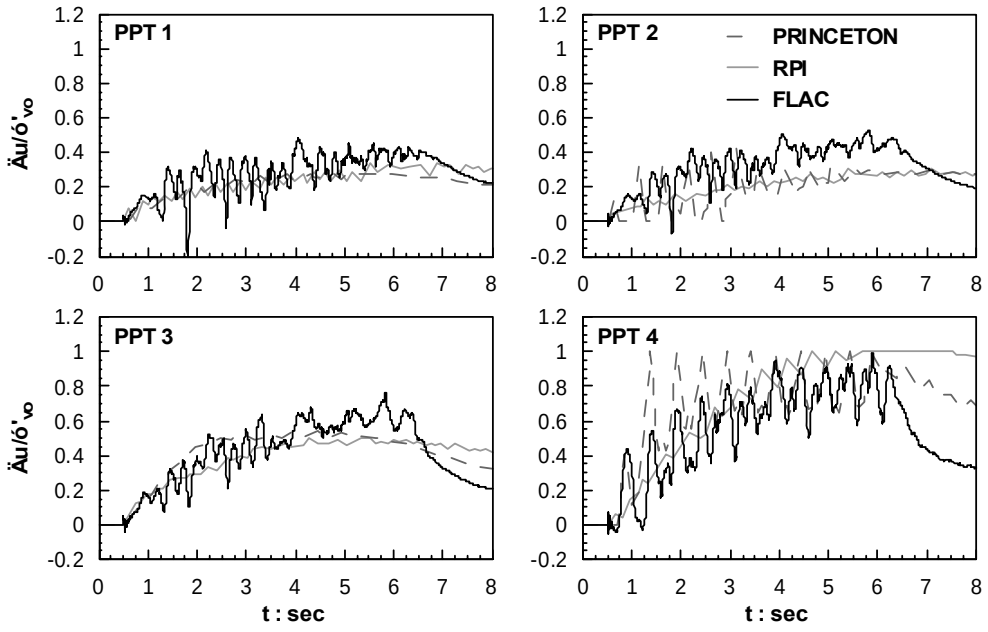

Figure 12 Comparison of excess pore pressure ratio time histories from analysis and centrifuge tests at various locations under the structure (PP1, PP2, PP3) and at free field (PP4)

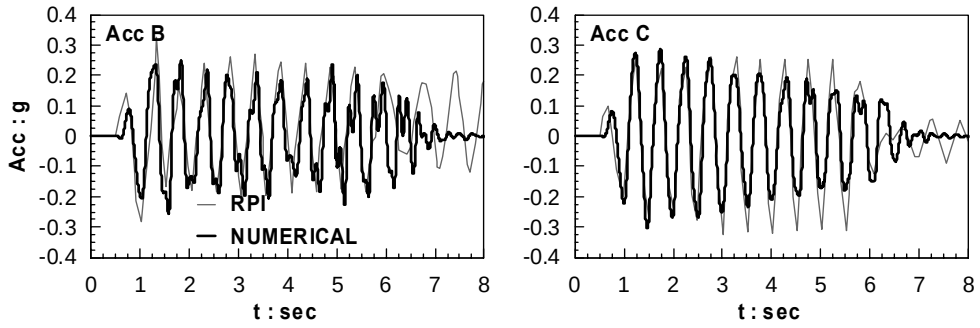

Figure 13 Comparison of acceleration time histories from analysis and centrifuge test at various depths below the structure

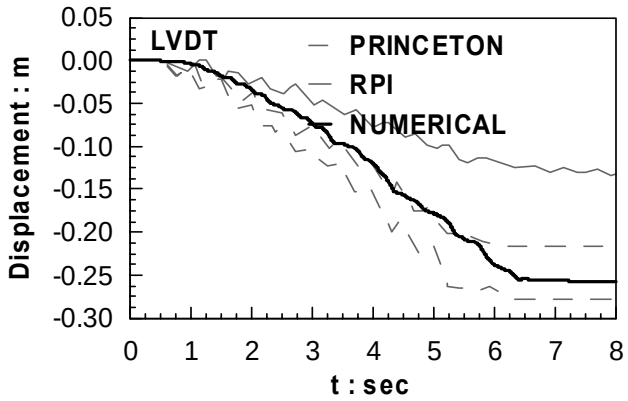

Figure 14 Comparison of structure settlement from analysis and centrifuge tests

As it can be seen, the numerical methodology predicts with quite satisfactory accuracy the centrifuge results. The only point of deviation between numerical and experimental results is the rate of excess pore pressure dissipation at the end of shaking, with predicted rates being higher that recorded ones. One possible explanation for this observed difference is the approximate simulation of the real input motion, which continues with reduced

amplitude even after 6 seconds of shaking. This part of the input motion was not taken into account during the numerical analyses (Fig. 10) for reasons of simplicity. Predicted and recorded seismic accelerations and permanent displacements are compared in Figures 13 & 14. Observe that the numerical results are reasonably close to the centrifuge results, suggesting that the proposed methodology simulates correctly the observed ground and foundation shaking.

Further details from this comparison can be found in Andrianopoulos (2006). What is of most importance is that this level of accuracy has been achieved for VELACS Model tests No. 1 and 2, as well, and this with the same set of model constants for all (3) distinctly different boundary value problems.

6. RESPONSE OF SHALLOW FOUNDATIONS ON A LIQUEFIABLE SOIL LAYER

Despite the severity of damages observed in various earthquakes (starting from the Niigata 1964 earthquake), relatively little has been achieved towards the development of a consistent methodology for the design of shallow foundations on a liquefiable layer. Usually, the presence of a superstructure is neglected and calculations are performed for free-field conditions. The onset of liquefaction is evaluated and empirical correlations for settlements, developed for free-field conditions, are used. However, the presence of a superstructure differentiates significantly the response from that under free-field conditions (e.g. compare the response in PPT2 and PPT4 in Figure 12), so that such methods are practically too crude.

Having built confidence on the proposed numerical methodology, the practical problem of a shallow footing resting on a liquefiable sand layer with a non-liquefiable clay cap is investigated numerically. This paper presents results from preliminary analyses that were performed for a uniform clay cap with an undrained shear strength S_u = 40kPa resting on a Nevada sand with D_r = 50%. The use of Nevada sand as the liquefiable material implies the use of the model constants calibrated in section 4 of this paper. The clay was simulated using the built-in Mohr-Coulomb model with c = 40kPa and $\varphi = 0^o$. The width of the footing is taken as B = 4m, while the thickness of the clay cap H was initially set equal to B. The finite difference mesh was subjected to a dynamic excitation, applied on the base of the sand layer. The input motion consists of a Chang's signal with peak acceleration equal to 0.25g, and shaking time approximately 3 sec. As a reference case, the problem of the static response of the same configuration was also simulated. In both the static and dynamic analyses, the footing was loaded with 130kPa, a value corresponding to a Safety Factor equal to 2 under static conditions. Figure 15 presents the deformed mesh and the shear strain increment contours (dark areas denote high levels) from the two (2) foregoing analyses.

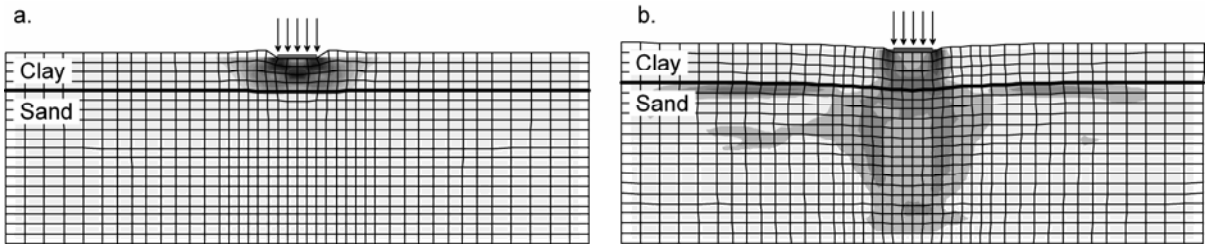

Figure 15 Deformed mesh and shear strain rate contours indicating the mode of failure under (a) static and (b) dynamic conditions

As deduced from Figure 15a, failure due to static loading is shown to occur inside the clay cap. On the other hand, Figure 15b shows that the mechanism of failure after liquefaction of the sand layer, is quite different. A punch-through type failure is observed within the clay cap and the underlying sand, where the shear strain rate contours indicate the formation of a practically orthogonal prism underneath the footing. Liquefaction of the surrounding soil seems to reduce this block's lateral support and result in the accumulation of large vertical strains. In fact, for the case of H = B = 4m, liquefaction of the sand layer resulted in the development of settlements equal to 15.6cm.

The above failure mechanism due to liquefaction resembles the one assumed by the analytical method of Bouckovalas et al. (2005), where the bearing capacity of the sand layer degrades gradually as a function of pore pressures development. Furthermore, this type of punch-through failure has been observed in numerous earthquakes, and is typical of buildings with a relatively low height over width ratio that settle significantly with

little deviation from verticality. This promising qualitative result enabled a set of parametric analyses for a variable clay cap thickness H, whose preliminary results can be found in Andrianopoulos et al (2006).

7. CONCLUSIONS

It may be concluded that the proposed constitutive model predicts with accuracy the stress-strain response of non-cohesive soils (sands and silts) during loading:

- at element level, as well as in complex boundary value problems,
- under small, medium and large strain amplitudes,
- for monotonic and cyclic conditions,
- under drained and undrained conditions, and
- for various soil densities, stress levels and loading directions.

From a practical point of view, the most important asset of the proposed methodology is that for all aforementioned conditions, a single soil-specific set of model constants is needed. Furthermore, it has been shown that the proposed implemented UDM in *FLAC* is a promising numerical tool for performing realistic, fully-coupled dynamic analyses for practical problems of Geotechnical Earthquake Engineering. Its use as a research tool for the practical problem of a shallow footing resting on a liquefiable layer is currently under way.

8. ACKNOWLEDGMENT

The work presented herein has been financially supported by the General Secretariat for Research and Technology (Γ.Γ.Ε.Τ.) of Greece, through research project ΕΠΑΝ – ΔΠ23 ("X-SOILS"). This contribution is gratefully acknowledged

9. REFERENCES

Andrianopoulos, K.I., (2006), Numerical modeling of static and dynamic behavior of elastoplastic soils. *Doctorate Thesis*, Department of Geotechnical Engineering, School of Civil Engineering, National Technical University of Athens (in Greek)

Andrianopoulos, K.I., Papadimitriou, A.G. and Bouckovalas, G.D., (2005), Bounding surface models of sands: Pitfalls of mapping rules for cyclic loading. *Proceedings, 11th International Conference on Computer Methods and Advances in Geomechanics*, Torino, June, Vol. 1: 241-248

Andrianopoulos, K.I., Bouckovalas, G.D., Karamitros D.K., Papadimitriou, A.G., (2006), Effective stress analyses for the seismic response of shallow foundations on liquefiable sand, *Proceedings, 6th European Conference on Numerical Methods in Geotechnical Engineering*, Graz, September, (in press)

Arulmoli, K., Muraleetharan, K.K., Hossain, M.M. and Fruth, L.S., (1992), VELACS: verification of liquefaction analyses by centrifuge studies; Laboratory Testing Program – Soil Data Report, *Research Report*, The Earth Technology Corporation.

Been, K. & Jefferies, M.G., (1985), A state parameter for sands. *Geotechnique*, 35, no.2, 99-112

Bouckovalas G.D, Valsamis, A.I. and Andrianopoulos, K.I., (2005), Pseudo static vs perfomance based seismic bearing capacity of footings on liquefiable soil, *Proceedings of the TC4 Satellite Confer., 16th International Conference on Soil Mechanics and Geotechnical Engineering*, Osaka, September, pp. 22-29

Hueckel, T. and Nova, R., (1979), Some hysteresis effects of the behavior of geological media, *International Journal of Solids and Structures,* 15, 625-642.

Itasca Consulting Group, Inc., (1998), FLAC – Fast Lagrangian Analysis of Continua, Version 3.4, *User's Manual*, Minneapolis: Itasca

Naylor, D.J., (1985), A continuous plasticity version of the critical state model, *International Journal of Numerical Methods in Engineering*, 21: 1187-1204.

Papadimitriou, A.G., Bouckovalas, G.D. and Dafalias, Y.F., (2001), Plasticity model for sand under small and large cyclic strains, *Journal of Geotechnical and Geoenvironmental Engineering*, ASCE, 127, no. 11, 973-983.

Papadimitriou, A.G. and Bouckovalas, G.D., (2002), Plasticity model for sand under small and large cyclic strains: a multiaxial formulation, *Soil Dynamics and Earthquake Engineering*, 22, 191-204.

Sloan, S.W., Abbo A. J., Sheng D. (2001), Refined explicit integration of elastoplastic models with automatic error control, *Engineering Computations,* 18 (1/2), 121-154